Title
Constitutive Model for the Undrained Compression of Unsaturated Clay

Journal
Journal of Geotechnical and Geoenvironmental Engineering, 143(4)

ISSN
1090-0241

Authors
Mun, Woongju
McCartney, John S

Publication Date
2017-04-01

DOI
10.1061/(asce)gt.1943-5606.0001635

Peer reviewed

CONSTITUTIVE MODEL FOR THE UNDRAINED COMPRESSION OF UNSATURATED CLAY

by Woongju Mun, M.S., S.M. ASCE[1] and John S. McCartney, Ph.D., P.E., M. ASCE[2]

Abstract: This paper proposes a constitutive model to describe the isotropic compression response of unsaturated, compacted clay under undrained conditions over a wide range of mean stresses. The total stress-based model captures the impacts of the initial degree of saturation on the apparent preconsolidation stress and the slope of the compression curve up to the point of pressurized saturation. The points of pressurized saturation for specimens with different initial degrees of saturation were predicted using a modified form of Hilf's pore pressure analysis. The compression response for pressure-saturated specimens was dominated by the pore water, although dissolved air and soil structure may play a role for some soils. The model was calibrated using results from a series of compression tests on compacted clay specimens having initial degrees of saturation ranging from 0.6 to 1.0 and the same initial void ratio. The model was found to provide a good match to the experimental data for mean stresses up to 160 MPa, in particular due to the improvements in Hilf's analysis to evaluate the points of pressurized saturation.

INTRODUCTION

Although the highest mean stresses encountered in geotechnical applications such as embankment dams and deep tunnels is on the range of 10 MPa, higher mean stresses may be encountered in the evaluation of buried explosives, impact loading, and hydraulic fracturing. Despite the mature understanding of these different topics, the isotropic compression response of soils under undrained conditions remains a complex subject that has not received significant

[1] Doctoral Candidate, University of Colorado Boulder, Dept. of Civil, Environmental and Architectural Engineering, UCB 428, Boulder, CO 80309; woongju.mun@colorado.edu

[2] Associate Professor, University of California San Diego, Department of Structural Engineering. 9500 Gilman Dr., La Jolla, CA 92093-0085, mccartney@ucsd.edu.

attention. This is perhaps because the undrained compression of saturated soil is often assumed to be dominated by the compression response of water, except in the case of very stiff soils (Skempton 1961). This same assumption cannot be made for unsaturated soils, as the presence of air-filled voids may have a significant impact on the compression response of soils over a wide range of mean stresses. In the other extreme, the undrained compression of dry soils can be safely assumed to be similar to their drained compression response (Mun and McCartney 2016). Although it may be useful to interpret undrained tests using an effective stress analysis in order to define fundamental material properties, effective stress analyses are focused on volume changes of the soil skeleton and cannot estimate the changes in volume of the bulk soil-water mixture due to the finite compressibility of water. Due to these issues, some models involve the use of total stress analysis to evaluate the compression response of soils in undrained conditions (e.g., Zimmerman et al. 1987). However, a model that is based on total stress analysis alone may not capable of capturing the fundamental mechanisms governing the compression response of unsaturated soils, where the magnitude of pore water pressure generation and compressibility of the soil skeleton during undrained loading depend on the initial degree of saturation. Accordingly, concepts from effective stress analyses can be used to obtain an undrained compression model in terms of total stress that can be applied to both saturated and unsaturated soils compressed to high stresses.

This paper seeks to define a constitutive model for the isotropic compression of unsaturated, compacted soils to mean stresses greater than 100 MPa under undrained conditions in terms of total stress. The model is built around a modified form of the pore pressure analysis of Hilf (1948), which is used to estimate the changes in pore air and water pressures during undrained compression. Further, the modified form of Hilf's analysis is useful to estimate the mean total stress required to reach pressurized saturation of an initially unsaturated specimen. Other aspects of the model were developed using the results from a series of isotropic, undrained compression tests on unsaturated, compacted clay specimens having initial degrees of saturation ranging from 0.6 to 1.0 but with the same initial void ratio. These tests were performed following the testing methodology described by Mun and McCartney (2015), with an extension to a wider range of initial conditions.

BACKGROUND

Undrained Compression of Unsaturated Soils to High Stresses

Hypothetical isotropic compression curves for unsaturated, compacted clay under undrained conditions are shown in Figure 1, based on the observations from preliminary tests performed by Mun and McCartney (2015). The initial compression of compacted, unsaturated clay follows an elastic recompression line until reaching a mean apparent preconsolidation stress p_c. Although the slope of the RCL of unsaturated specimens may be slightly greater than that of saturated specimens in undrained compression, the effect of suction on the slope of the RCL is negligible (Points A to B). The value of p_c is dependent on the initial compaction conditions, which not only leads to potentially different soil structures but also different initial suction values. The initial suction in compacted soils may lead to an apparent suction-induced hardening in a similar manner to that observed in drained compression tests (Alonso et al. 1990). After passing the mean apparent preconsolidation stress, the slopes of undrained compression curves for unsaturated soils (Points B to C) increase with decreasing initial degrees of saturation. The pore air is expected to dissolve into the water at the point of pressurized saturation (Point C). Although continued particle rearrangements and crushing could occur at very high stresses, continued deformation is primarily expected due to elastic compression of the water (Points C to D), after the point of pressurized saturation (Skempton 1961; Mun and McCartney 2015). Mun and McCartney (2016) observed that particle breakage occurred in undrained compression tests on saturated sand to mean total stresses of 160 MPa, even though the shape of the compression curve was mainly dominated by the compression of the pore water. Little data is available for particle breakage in finer-grained soils compressed to high stresses, although the same magnitude of grain crushing observed in sands is likely not to occur for the smaller, more flexible particles in clay soils. In addition to particle breakage, the amount of air dissolved in the pore water may affect the compressibility of water, affecting the undrained compression response of the pressure-saturated specimens.

Pore Pressure Generation in Unsaturated Soils during Undrained Compression

Several experimental studies have investigated the changes in pore air and water pressures during undrained compression (Hilf 1948; Bishop 1960; Bishop et al. 1960; Bishop and Henkel 1962; Gibbs et al. 1960; Gibbs 1963; Barden and Sides 1970; Campbell 1973; Hakimi et al. 1973; Penman 1978; Rahardjo 1990; Rahardjo and Fredlund 1995). In general, these studies observed that both pore air and water pressures increase with increasing total stress until reaching the point of pressurized saturation, at which point the air is no longer present and the pore water pressure increases proportionally to the total stress. Hilf (1948) assumed that the pore air and water pressures increase by the same amount during undrained compression, meaning that the matric suction does not change significantly. In reality, the pore water pressure is initially lower than the pore air pressure in unsaturated soils so the two pore pressures must change by different amounts and converge at some point. Bishop and Donald (1961) showed experimental data of pore air and water pressures during isotropic compression of compacted clay up to mean stresses of 0.83 MPa, and observed that the changes in pore air and water pressures slowly converge during compression, with a rate of convergence that is greater for specimens with higher initial degrees of saturation, and that most of the changes in matric suction occur below mean total stresses of 0.2 MPa for their soil. This may be due to the initial compression of the air-filled voids before the pore air starts to dissolve into the pore water. Hasan and Fredlund (1980) compared different models to estimate the changes in pore air and pore water pressures during undrained compression with experimentally-measured data. They suggested that it is important to independently predict changes in pore air and pore water pressures for highly compressible soils, indicating that changes in matric suction may affect the compression of these materials. However, for stiffer soils such as overconsolidated soils and those prepared using compaction it is safe to assume that changes in pore air and water pressure are equal during undrained compression, and the assumption of Hilf (1948) is valid. Further, they found that it may be appropriate to consider that the compressibility of the soil skeleton changes with total stress, while previous studies such as Bishop et al. (1960) and Gibbs (1963) had assumed a constant compressibility.

Hilf (1948) combined Boyle's law and a simplified form of Henry's law to estimate the change in pore air pressure expected during changes in porosity under undrained conditions. He noted that his analysis could be combined with an elastic analysis of the volumetric strain to estimate the change in pore air pressure during a change in mean total stress, which was later presented in equation form by Fredlund and Rahardjo (1993). A major assumption in Hilf's analysis is that the volume of dissolved air in the water is constant, which simplified the calculations of the change in air pressure. Despite the fact that this assumption is not physically realistic, Hasan and Fredlund (1980) found that the analysis of Hilf (1948) provides a good estimation of the pore pressure in the case where the soil has a highly rigid structure and the initial matric suction is low. Further, Rahardjo (1990) found that simultaneous measurements of pore air and pore water pressures during oedometer tests on unsaturated soils under undrained or constant water content conditions agreed well with the predictions from the analysis of Hilf (1948). Although the model of Hilf (1948) has been shown to be useful, the assumption of a constant volume of dissolved air does not permit evaluation of the case of pressurized saturation. At the point of pressurized saturation during undrained compression to high stresses, the free pore air will be completely dissolved into the pore water. Schuurman (1966) developed an equation to predict the pore water pressure required to reach pressure saturation, focusing on the case where additional pore water is supplied to the specimen to compress the pore air, a process commonly referred to as backpressure saturation. However, Schuurman (966) also assumed that the volume of dissolved air did not depend on the applied pressure. Accordingly, the pore pressure analysis of Hilf (1948) needs to be updated to consider pressurized saturation during undrained compression.

MODIFIED HILF ANALYSIS FOR PRESSURIZED SATURATION

This section presents a derivation similar to the analysis of Hilf (1948) to predict the changes in pore water pressure during undrained compression, with consideration of the process of pressurized saturation. According to Henry's law, the solubility of air in water (h) is proportional to the pore air pressure u_a (i.e., $h = u_a/k_h$, where k_h is a constant coefficient of proportionality). As the solubility can be expressed in terms of a volumetric concentration (Lu and Likos 2004), the volume of dissolved air V_d in a unit volume of water V_w can be expressed as follows:

$$V_d = h \cdot V_w = \left(\frac{u_a}{k_h} \right) \cdot V_w \tag{1}$$

where k_h is Henry's law constant. Equation 1 requires the use of the absolute air pressure ($u_a = u_{a,absolute} = 101.3$ kPa at 20 °C), so the air pressure in this study is considered in absolute terms for all of the analyses. This is an important point to make as it is common to use gauge pressure ($u_{a,gauge} = 0$ kPa) in geotechnical engineering analyses of unsaturated soil problems. In Hilf's analysis, the initial pressure in both the free and dissolved air is assumed to be at atmospheric conditions (i.e., u_{a0} = 101.3 kPa). Under atmospheric pressure, the solubility h ranges from 0.0235 to 0.0201 for temperatures ranging from 10 to 20 °C (Gibbs et al. 1960), which implies that the value of k_h is equal to approximately 5628 kPa at a temperature of 20 °C.

It is possible to re-derive the pore water pressure analysis of Hilf (1948) using the form of Henry's law in Equation (1). According to Boyle's law, the product of the pore air pressure and volume of pore air is constant for a given mass of confined air ($u_a V_a$=constant). Further, Hilf (1948) assumed that dissolved air also follows Boyle's law, which implies that the dissolved air is still compressible and can be considered as an ideal gas. Accordingly, the total mass of free and dissolved air in the undrained specimen is considered using Boyle's law. This is a key simplifying assumption that is necessary to evaluate the complex process of pressurized saturation. Another assumption is that the reduction in soil volume is only assumed to be the result of the compression of free air, the dissolved air, and the soil skeleton, while it is assumed that the soil solids and the water are incompressible. When the pore water is assumed to be incompressible, the volume of water in the soil during undrained compression is constant (i.e., V_{wf} = V_{w0}). Following these assumptions, Boyle's law can be written in terms of the initial and final volumes of the free and dissolved air, and the initial pore air pressure u_{a0} and the final pore air pressure (u_{a0}+Δu_a), as follows:

$$\left(V_{a0} + h_0 \cdot V_{w0}\right) \cdot u_{a0} = \left(V_{af} + h_f \cdot V_{w0}\right) \cdot \left(u_{a0} + \Delta u_a\right) \quad (2)$$

where V_{a0} and V_{af} are the initial and final volumes of free air, respectively, h_0 and h_f are the initial and final values of the solubility of air in water, and V_{w0} is the initial volume of water which is equal to the final volume of water V_{wf} during undrained compression. Equation (2) differs from that of Hilf (1948) in that the initial volume of dissolved air is $h_0 V_{w0}$, while the volume of dissolved air after compression will be $h_f V_{w0}$. The value of h will increase with changes in pore air pressure, implying that more air is dissolved in the pore water under increasing pressure following Equation (1). During compression of an unsaturated soil, a reduction in the volume of voids (ΔV_v) can be assumed to be equal to the change in the volume of free air (i.e., $V_{af} = V_{a0} + \Delta V_v$). Based on this assumption, the following relationship can be obtained from Equation (2) by dividing the first and second terms by the volume of voids (V_{v0}):

$$\left[(1-S_{r0})\cdot n_0 + \frac{u_{a0}}{k_h}\cdot S_{r0}\cdot n_0\right]\cdot u_{a0} = \left[(1-S_{r0})\cdot n_0 + \Delta n + \frac{u_{a0}+\Delta u_a}{k_h}\cdot S_{r0}\cdot n_0\right]\cdot\left(u_{a0}+\Delta u_a\right) \qquad (3)$$

where n_0 is the initial porosity, Δn is the change in porosity ($\Delta V_v/V_t$), and S_{r0} is the initial degree of saturation (V_w/V_v). The volume of free air in the soil V_{a0} is equal to $(1-S_{r0})\cdot n_0$ and the volume of dissolved air is hS_rn_0.

Rearranging Equation (3) represents an expression for the change in porosity (Δn), as follows:

$$\Delta n = -\left[\frac{(1-S_{r0})\cdot n_0\cdot\Delta u_a + \frac{S_{r0}\cdot n_0}{k_h}\cdot\left(\Delta u_a^2 + 2\Delta u_a\cdot u_{a0}\right)}{\left(u_{a0}+\Delta u_a\right)}\right] \qquad (4)$$

At the point of pressurized saturation, all of the free air has been dissolved into the water and the change in porosity should be equal to the initial volume of free air (i.e., $V_{a0} = (1-S_{r0})\cdot n_0$). Following this assumption, the change in pore air pressure required to reach pressurized saturation ($\Delta u_{a,ps}$) can be estimated as follows:

$$\left(\frac{S_{r0}}{k_h}\right)\Delta u_{a,ps}^2 + \left(2u_{a0}\frac{S_{r0}}{k_h}\right)\Delta u_{a,ps} - u_{a0}\left(1-S_{r0}\right) = 0 \qquad (5)$$

where $\Delta u_{a,ps}$ is one of the solutions of the quadratic equation. Because of the assumption of a constant volume of dissolved air, Hilf (1948) was able to directly solve for the change in air pressure at the point of pressurized saturation. However, Equation (5) is still relatively straightforward to calculate and better considers the physics of pressurized saturation.

Ideally, changes in volume of a soil should be calculated using a change in mean effective stress, which can be calculated using a form of Bishop's (1959) equation, given as follows:

$$\Delta p' = \left(\Delta p - \Delta u_a\right) + \left[\chi\left(\Delta u_a - \Delta u_w\right)\right] \tag{6}$$

where Δp is the change in mean total stress and χ is the effective stress parameter which can be assumed equal to the degree of saturation ($\chi = S_r$). The volume change behavior of unsaturated soil concepts can also be captured from constitutive models defined in terms of independent stress state variables (Alonso et al. 1990; Josa et al. 1992; Wheeler and Sivakumar 1995; Sheng et al. 2008). Hilf (1948) assumed that the matric suction of the soil does not significantly change during undrained compression, which implies that the change in pore air pressure (Δu_a) will be equal to the change in pore water pressure (Δu_w). In this case, Hilf (1948) estimated the volumetric strain of the soil skeleton as follows:

$$\frac{\Delta V_t}{V_t} = \Delta n = -m_v\left(\Delta p - \Delta u_a\right) \tag{7}$$

where the difference between Δp and Δu_a is the change in mean net stress and m_v is the coefficient of volume compressibility of soil, which can be defined for isotropic compression as follows:

$$m_v = \frac{1}{1+e_0}\frac{\Delta e}{\left(\Delta p - \Delta u_a\right)} \tag{8}$$

where e_0 is the initial void ratio. Although Equation (7) involves a simplified form of the effective stress in Equation (6), in many cases the pore air pressure is not known during compression making it difficult to define the value of m_v experimentally. Alternatively, the compression response of unsaturated soils under undrained conditions can be represented in terms of changes in mean total stress, as follows:

$$\frac{\Delta V_t}{V_t} = \Delta n = -m_{v,u} \Delta p \tag{9}$$

where $m_{v,u}$ is the coefficient of volume compressibility of soil in undrained conditions. This approach permits the overall changes in volume due to changes in externally applied mean total stresses to be obtained. As noted in the introduction, a total stress analysis such as this may be appropriate for the evaluation of volume changes of nearly saturated soils at high stresses. As the compression curves for most soils are nonlinear, $m_{v,u}$ will not be constant and will change with mean stress. In order to evaluate pressurized saturation, the value of $m_{v,u}$ should be defined between the mean apparent preconsolidation stress and the mean stress at the point of pressurized saturation. Following the hypothetical trends shown in Figure 1 it is expected that the value of $m_{v,u}$ in this range will depend on the initial degree of saturation.

By combining Equations (4) and (9), the change in pore air pressure during a change in mean total stress under undrained conditions can be rearranged as follows:

$$\left(\frac{S_{r0} n_0}{k_h}\right) \Delta u_a^2 + \left((1 - S_{r0}) n_0 + \frac{2 u_{a0} S_{r0} n_0}{k_h} - m_{v,u} \Delta p \right) \Delta u_a - m_{v,u} u_{a0} \Delta p = 0 \tag{10}$$

where the change in pore air pressure (Δu_a) during changes in mean total stress (Δp) under undrained conditions is one of the solutions of the quadratic equation.

In order to assess the points of pressurized saturation for soils having different initial degrees of saturation (S_{r0}) or coefficients of volume compressibility ($m_{v,u}$), a parametric evaluation of the modified Hilf analysis was performed. The change in pore air pressure required to reach the point of pressurized saturation ($\Delta u_{a,ps}$) calculated using Equation (5) for soils having different initial degrees of saturation is shown in Figure 2(a), along with the predictions from the analysis of Hilf

(1948). In this analysis, the initial air pressure was assumed to be atmospheric pressure (101.3 kPa), and the Henry's law constant k_h was 5628 kPa. In the equation of Hilf (1948), the volumetric coefficient of solubility (h) was assumed to be constant and equal to 0.02. Although the value of $\Delta u_{a,ps}$ is observed to increase nonlinearly with decreasing initial degrees of saturation in both analysis, the change in pore air pressure required to reach the pressure saturation is much lower for the modified Hilf analysis than those calculated using the analysis of Hilf (1948). This has major implications on the calculation of the points of pressurized saturation.

The changes in pore air pressure as a function of the change in mean total stress calculated using Equation (10) are shown in Figure 2(b). The values of $\Delta u_{a,ps}$ for each of the initial degrees of saturation are also shown in this figure. The intersections between the lines defined by Equations (5) and (10) provide the values of mean total stress required to reach pressurized saturation for soils having different initial degrees of saturation. However, the intersection points shown in Figure 2(b) do not consider the fact that soils with a lower initial degree of saturation may have a higher value of $m_{v,u}$. The changes in pore pressure with increasing mean total stress for soils having different values of $m_{v,u}$ are shown in Figure 2(c). The results in this figure indicate that greater changes in mean total stress are required to reach the point of pressurized saturation for stiffer soils that have a smaller value of $m_{v,u}$.

EXPERIMENTAL APPROACH

Materials and Specimen Preparation

A low plasticity clay referred to as Boulder clay was selected as the test material for this study. The clay has a liquid limit of 41, plastic limit of 18, and plasticity index of 23, so it can be classified as CL according to the Unified Soil Classification Scheme. The specific gravity G_s was measured to be 2.70. The maximum dry unit weight and optimal water content corresponding to the Standard

Proctor compaction effort are 17.4 kN/m^3 and 17.5%, respectively. Specimens having a diameter and height of 71.1 mm were prepared using static compaction to reach a target dry unit weight of 17.5 kN/m^3, which corresponds to an initial void ratio of 0.51. The specimens were prepared using different initial compaction gravimetric water contents to evaluate the role of the initial degree of saturation on the shape of the undrained compression curve. The achieved initial degrees of saturation and initial void ratios for the different specimens are shown in Table 1. It is acknowledged that compaction of specimens to different initial gravimetric water contents will lead to potentially different soil structures as well as different initial suction values. However, all of the specimens were compacted dry of optimum, so the soil structure is likely similar between the different specimens. It should be noted that the specimen having S_{r0} = 1.00 was prepared at the same conditions as the specimen having S_{r0} = 0.92, but was subsequently saturated by upward imbibition of water while applying a vacuum to the top of the specimen. After saturation, this specimen was placed under a backpressure of 210 kPa, and Skempton's B parameter was measured to be 0.97 before starting the undrained compression test.

The soil water retention curve (SWRC) for the Boulder clay specimen used in the compression tests were inferred using the Transient Water Release and Imbibition Method (TRIM) of Wayllace and Lu (2012). The initial suction values of each specimen were measured using a UMS T5 tensiometer applying procedures followed by Mun and McCartney (2015). The SWRC for Boulder clay is shown in Figure 3 along with the initial suctions from the tensiometer measurements, which were observed to fall onto the drainage path of the SWRC. The van Genuchten (1980) SWRC model parameters α_{vG} and n_{vG} are also shown in Figure 3.

High Pressure Isotropic Testing of Unsaturated Clay

A series of undrained isotropic compression tests under mean stresses up to 160 MPa were conducted for clay specimens having initial degrees of saturation with the same initial void ratio. The experiments were performed in a high pressure isotropic loading apparatus that uses a high-pressure syringe pump to control the total stress and track changes in specimen volume. This device was previously used by Mun and McCartney (2015), who presented detailed explanations of the different aspects of the device, system calibration, and testing procedures. After preparation of the compacted specimens and placement within the isotropic cell, mean total stresses were applied at a constant rate of 2%/hour using the syringe pump without permitting drainage from the specimen until reaching a mean total stress of 160 MPa. The rate selected in this study is relatively slow because the process of pressure saturation in unsaturated soils is expected to be a time-dependent process as noted by Schuurman (1966). The pore water and air pressure were not measured during these compression experiments as this would have required a special tensiometer that would be capable of resolving small differences in pore air and water pressures at small suctions as well as high pressures potentially up to 160 MPa. Further, measurement of pore air pressures that are representative of occluded air bubbles is also a complex subject. Nonetheless, it was still possible to infer the point of pressurized saturation from the volume change versus mean total stress plots.

Experimental Results

A series of undrained isotropic compression tests were conducted with different initial degrees of saturation ranging from 1.0 to 0.6 under the mean stresses up to 160 MPa. The undrained compression curves with various initial degrees of saturation plotted on logarithm of mean stresses are shown in Figure 4(a). The results seem that the initial response for the unsaturated specimens is controlled by soil structures and the presence of air-filled voids lead to a softer response to ascend, until it reaches the apparent pressurized saturation. Evaluation of the compression curves indicates that the mean apparent preconsolidation stress (p_c) increases with decreasing initial degrees of saturation. Furthermore, the slopes of undrained compression curves of unsaturated soil become steeper with decreasing initial degrees of saturation which reflects the compression of the air-filled voids. The undrained compression curves are shown with the mean stresses on a natural scale in Figure 4(b) for further assessment of the trends in the data. On these plots, the initial slopes of the undrained compression curves are observed to increase with decreasing initial degree of saturation, and bends in the curves are observed at a point that likely corresponds to the point of pressurized saturation. For mean stresses greater than the bends in the curves, the undrained compression curves are approximately linear with increasing mean stress.

In order to verify the points of pressurized saturation from the undrained compression curves, the initial volume of air $V_{a,i}$ in each clay specimen is compared with the volume of voids at the bends in the curves $V_{v,ps}$ in Figure 5. The comparison follows a 1:1 relationship confirming that the initial compression response is associated with the volume change of the air-filled voids. However, the changes in the volume of voids at the points of pressurized saturation are slightly less than the initial volume of air in the void of unsaturated soil, which may be due to the dissolution of air into the pore water.

UNDRAINED COMPRESSION MODEL FOR UNSATURATED CLAY

The undrained compression curves from the experiments indicate that the unsaturated soils exhibit elastic behavior until reaching a mean apparent preconsolidation stress (p_c), which appears to depend on the initial compaction conditions and potentially the presence of suction. In this case, the slope of the RCL of the unsaturated specimen in undrained compression line may be slightly greater than that of saturated soil. Changes in void ratio (e) in this elastic region (Section A-B in Figure 1) can be expressed as follows:

$$\Delta e = \kappa_{u,i} \cdot \ln \frac{p_c}{p_0} \tag{11}$$

where $\kappa_{u,i}$ is the initial recompression index and p_0 is the initial total stress. The value of $\kappa_{u,i}$ for unsaturated soil was observed to be a bit greater than that of saturated soil, regardless of the different initial degree of saturation. A value of $\kappa_{u,i}$ equal to 0.0015 fit well for the saturated specimen and a value of $\kappa_{u,i}$ equal to 0.003 was found to fit well to all of the unsaturated specimens.

Although the mean apparent preconsolidation stress is observed to increase with decreasing initial degree of saturation in a similar manner to suction-induced hardening phenomena in drained tests, the trend in p_c may also be influenced by the soil structure induced by compacting the specimens dry of optimum. However, as it is difficult to quantify the role of soil structure, an empirical relationship between the value of p_c and the initial degree of saturation was defined based on the trends in the data, as shown in Figure 6(a). The following expression was defined for the trends in mean preconsolidation stress for undrained compression:

$$p_c = A \ln\left(S_{r0}\right) + B \tag{12}$$

where A and B are fitting parameters, which were found to equal -825 and 198 kPa for Boulder clay using least-squares optimization. The simple log-linear relationship was found to match well with the initial degree of saturation for the compacted soils. It should be noted that loading-collapse (LC) curves available in the literature such as that of Alonso et al. (1990) could not be used because the suction is not necessarily constant during undrained compression of the unsaturated soil.

After reaching the mean apparent preconsolidation stress, the unsaturated specimens are observed to decrease in volume depending on the quantity of the initial air-filled voids, which is related inversely to the degree of saturation. The undrained compression response of the unsaturated soils after the mean apparent preconsolidation stress can be calculated as follows:

$$\Delta e = \lambda_{u,i} \cdot \ln \frac{p_{ps}}{p_c} \tag{13}$$

where $\lambda_{u,i}$ is the slope of the undrained compression curves of unsaturated soil after the mean preconsolidation stress. The slopes of this portion of the undrained compression curves were assessed from the experimental data in Figure 4(a), and an empirical relationship was defined by plotting these slopes against the initial degree of saturation in Figure 6(b). The following relationship was defined from the data:

$$\lambda_{u,i} = Z \cdot \ln(S_{r0}) \tag{14}$$

where Z is a fitting parameter. It should be noted that the saturated specimens do not show a change in slope after reaching the preconsolidation stress, so Equation (14) gives a value of $\lambda_{u,i}$ of 0 for saturated soils. This implies that the volume change calculated using Equation (13) for saturated soils will be zero. For the unsaturated specimens, Equation (13) is valid until reaching the change in mean total stress required to reach the point of pressurized saturation Δp_{ps}, which can be calculated by combining Equations (5) and (10), as follows:

$$\Delta p_{ps} = \frac{(1 - S_{r0}) n_0 \Delta u_{a,ps} + \dfrac{S_{r0} n_0}{k_h} \left(\Delta u_{a,ps}^2 + 2 \Delta u_{a,ps} u_{a0} \right)}{m_{v,u} \left(\Delta u_{a,ps} + u_{a0} \right)} \tag{15}$$

The values of $m_{v,u}$ in this equation can be obtained from the plot of the change in void ratio versus the change in the mean total stress shown in Figure 4(a). In this case, the value of $m_{v,u}$ in this equation is directly related to the value of $\lambda_{u,i}$ given in Equation (11), as follows:

$$m_{v,u} = \lambda_{u,i}\left[\frac{\ln 10 \cdot \log_{10}\left(\frac{p}{p_c}\right)}{(p - p_c)\cdot(1+e_0)}\right] \tag{16}$$

Similar to the value of $\lambda_{u,i}$, the value of $m_{v,u}$ is approximately zero for saturated soils, in which case the value of Δp_{ps} derived from Equation (15) is technically indeterminate. However, the value of $m_{v,u}$ of saturated soils is in reality slightly greater than zero during undrained compression as will be discussed below, so the value of Δp_{ps} in Equation (15) can be assumed to be zero for saturated soils. An assessment of the change in pore air pressure for specimens having different initial degrees of saturation using Equation (10) is shown in Figure 7(a) [using the trend in $m_{v,u}$ with S_{r0} obtained by combining Equations (14) and (16)]. This plot shows how the model is able to unify the effects of S_{r0} and $m_{v,u}$ observed in Figures 2(b) and 2(c). The experimental points of pressurized saturation for Boulder clay observed from the changes in slopes of the compression curves in Figure 4 are compared with the smooth function obtained from Equation (14) in Figure 7(b), indicating an excellent fit.

The results in Figure 4(b) indicate that the undrained compression curve for saturated soil is nearly linear when plotted on a natural scale. As the compression of the soil is potentially controlled by the pore water and the soil skeleton (Section B-D in Figure 1), the following model can be adopted for void ratio changes under mean total stresses above the point of pressurized saturation:

$$\Delta e = e_{ps} - \frac{(1+e_{ps})}{\alpha_u K_w}(p - p_{ps}) \tag{17}$$

where e_{ps} is the void ratio at the point of pressurized saturation (equal to the void ratio at yielding for saturated soil), K_w is the bulk modulus of pure water (2.2 GPa), and α_u is a coefficient that accounts for both the softer response of water with dissolved air and the potentially stiffer response of some soils than water. The α_u coefficient was incorporated because the slopes of the undrained compression curves for the unsaturated specimens in Figure 4 were observed to increase slightly with mean total stress but later approach that of water at high stresses. Accordingly, the value of α_u is assumed to be a function of the applied mean total stress and can be expressed as follows:

$$\alpha_u = \left(A^u \cdot \sqrt{(1-S_{r0})} + 1\right) - \left(A^u \cdot \sqrt{(1-S_{r0})}\right) \cdot \left(\frac{K}{K_w} - e^{\frac{-p}{(1+S_{r0})\times 10^5}}\right) \tag{18}$$

where K is the maximum bulk modulus of the soil, and A^u is a fitting parameter. The value of A^u was found to equal -0.7 for Boulder clay by manual fitting to the slopes of the compression curves for the unsaturated specimens. It should be noticed that the value of α_u is approximately equal to 1.0 for saturated soils that have the same bulk modulus as water ($K=K_w$). In addition to being sensitive to the initial degree of saturation, α_u is sensitive to the applied mean total stress, which will affect the role of the dissolved air in the bulk modulus of the water. The pressure effect was assumed to follow an exponential trend, and the pressure effect was damped by dividing by a constant value of 10^5. It was found that $K = K_w$ for Boulder clay, but this parameter is incorporated in case a soil is investigated that has a bulk modulus greater than that of water, a case that was observed for saturated sand by Mun and McCartney (2016). In this case, a higher value of K than K_w can be selected. The changes in the coefficient parameter α_u with applied pressure after pressurized saturation are shown in Figure 8. The trends in the curves reflect that the bulk modulus of pressure-saturated unsaturated soils will be initially be lower for lower initial degrees of saturation due to the amount of dissolved air into pore water, but will increase and approach that of water at high mean total stresses (i.e., α_u approaches 1).

The overall model for prediction of the undrained compression curve of saturated and unsaturated soils up to high stresses is summarized as follows:

$$\Delta e = e_0 - \kappa_{u,i} \cdot \ln \frac{p_c}{p_0} + \lambda_{u,i} \cdot \ln \frac{p_{ps}}{p_c} - \frac{\left(1 + e_{ps}\right)}{\alpha_u K_w}\left(p - p_{ps}\right) \tag{19}$$

As mentioned, the third term will be equal to zero for saturated soils, but otherwise this equation applies to both saturated and unsaturated soils. The initial degree of saturation plays an important role in the values of p_c and $\lambda_{u,i}$ for compacted soils, and also is useful in estimating the mean stress at the point of pressurized saturation p_{ps}.

EVALUATION OF MODELED COMPRESSION CURVES

The parameters of the model were defined to fit the undrained compression curves of the compacted specimens of Boulder clay shown in Figure 4. The model parameters are summarized in Table 2. The relationships for p_c and $\lambda_{u,i}$ from Figures 6(a) and 6(b), respectively, were used in the model, and the actual initial conditions (e.g., S_{r0}, e_0, p_0) from the experiments shown in Table 1 were used as model inputs. Comparisons between the model predictions (dashed lines) and the measured compression curves (solid lines) are shown in Figures 9(a) and 9(b) for specimens having different initial degrees of saturation, on logarithmic and natural scales, respectively. The model matched the experimental data well at high degrees of saturation. Especially, the model captures the nonlinear behavior at high stresses, which is induced by dissolved air for unsaturated conditions. The same model predictions are shown in Figures 9(c) and 9(d) on logarithmic and natural scales, respectively, without the experimental data to better observe the trends in the curve with the initial degrees of saturation. The model requires a total of 8 parameters, although the model could be simplified by using $\alpha_u = 1$ and neglecting the effect of the changes in bulk modulus of the pressure saturated specimens with increasing pressure. This is especially the case for applications that do not necessarily involve mean total stresses commonly used in geotechnical applications (10 MPa).

CONCLUSIONS

To characterize the undrained compression responses of unsaturated clay, a series of isotropic compression tests were performed on compacted specimens having different initial degrees of saturation up to a mean total stress of 160 MPa. A constitutive model was developed to characterize different transition points observed in the experimental data, using pore water pressure predictions from a modified version of the pore pressure analysis of Hilf (1948). During undrained compression, all compacted specimens initially followed the elastic compression response until reaching a mean apparent preconsolidation stress. Two different values slope of RCL were selected for saturated and unsaturated soil to represent the initial undrained compression response of Boulder clay, regardless of suction magnitude. Suction-induced hardening effects were observed in the undrained compression of unsaturated soil, although this trend was not as significant as observed in drained compression curves. Specimens with lower initial degrees of saturation show a softer compression response initially, although they have a stiffness that approaches that of saturated specimens at high mean total stresses. The mean total stress at the point of pressurized saturation from the experiments was found to be consistent with the predicted values from the modified version of the Hilf (1948) analysis, further proving the utility of this equation for use in evaluating unsaturated soil behavior. The compression response of unsaturated soils at high stresses beyond the point of pressurized saturation was observed to be sensitive to the amount of dissolved air in the pore water. Overall, the model was observed to provide a good match to the undrained compression curves for unsaturated soils with different initial degrees of saturation over a wide range of mean total stresses.

ACKNOWLEDGMENTS

Funding for this research was provided by Office of Naval Research (ONR) grant N00014-11-1-0691. The opinions in this paper are those of the authors alone.

APPENDIX I. REFERENCES

Alonso, E.E., Gens, A., and Josa, A. (1990). "A constitutive model for partly saturated soils." Géotechnique, 40(3), 405-430.

Barden, L. and Sides, G.R. (1970). "Engineering behavior and structure of compacted clay." Journal of the Soil Mechanical and Foundation Engineering Division. 96(3), 1171-1200.

Bishop, A.W. (1960). "The measurement of pore pressure in the triaxial test." Proceedings of Conference on Pore Pressure and Suction in Soils, Butterworth, London, 52-60

Bishop, A.W., Alpan, I., Blight, G., and Donald, I. (1960). "Factors controlling the strength of partly saturated soils." Proceedings of ASCE Research Conference on Shear Strength of Cohesive Soils, Boulder, CO, 503-532.

Bishop, A.W., and Donald, I. (1961). "The experimental study of partly saturated soil in the triaxial apparatus." Proceedings of the 5th International Conference on Soil Mechanics and Foundation Engineering, Paris, 13-21.

Bishop, A.W., and Henkel, D.J. (1962). The Measurement of Soil Properties in the Triaxial Test. 2nd edition, Edward Arnold Ltd., London.

Campbell, J.D. (1973). Pore Pressure Changes and Volume Changes in Unsaturated Soils. PhD Thesis. University of Illinois Urbana-Champaign.

Fredlund, D.G., and Rahardjo, H. (1993). Soil Mechanics for Unsaturated Soils. John Wiley & Sons, New York.

Gibbs, H.J., Hilf, J.W., Holtz, W.G., and Walker, F.C. (1960). "Shear strength of cohesive soils." ASCE Research Conference on Shear Strength of Cohesive Soils, University of Colorado, Boulder, CO, 33-162.

Gibbs, H.J. (1963). "Pore pressure control and evaluations for triaxial compressions." American Society for Testing and Materials, Special Technical Publication No. 361, 212-221.

Hakimi, Marchan, and Orliac. (1973). "Pore pressure in partly saturated soils, Prediction, Laboratory test and in-situ measurements." Proceedings of the 8th International Conference on Soil Mechanics and Foundation Engineering, Moscow, 163-170.

Hasan, J.U., and Fredlund, D.G. (1980). "Pore pressure parameters for unsaturated soils." Canadian Geotechnical Journal, 17(3), 395-404.

Hilf, J.W. (1948). "Estimating construction pore pressures in rolled earth dams." Proc. 2nd Int. Conference on Soil Mechanics and Foundation Engineering. Rotterdam, Vol. 3, 230-240.

Josa, A., Balmaceda, A., Gens, A., and Alonso, E. E. (1992). "An elastoplastic model for partially saturated soils exhibiting a maximum of collapse." Proc., 3rd International Conference on Computational Plasticity, Barcelona, Spain. 815-826.

Lu, N., and Likos, W.J. (2004). Unsaturated soil mechanics. John Wiley & Sons, New York.

Mun, W., and McCartney, J.S. (2015). "Compression mechanisms of unsaturated clay under high stress levels." Canadian Geotechnical Journal. 52, 1-14. 10.1139/cgj-2014-0438.

Mun, W., and McCartney, J.S. (2016). "Role of drainage in the compression of sand to high pressures." Journal of Geotechnical and Geoenvironmental Engineering. In review.

Penman, A.D.M. (1978). "Construction pore pressures in two earth dams." Building Research Establishment, Watford, U.K., 82-78.

Rahardjo, H. (1990). The Study of Undrained and Drained Behavior of Unsaturated Soils. Ph.D. thesis, Department of Civil Engineering, University of Saskatchewan.

Rahardjo, H. and Fredlund, D.G. (1995). “Experimental verification of the theory of consolidation for unsaturated soils.” Canadian Geotechnical Journal. 32(5), 749-766.

Schuurman, I.E. (1966). “The compressibility of an air/water mixture and a theoretical relation between the air and water pressure.” Géotechnique, 16(4), 269-281.

Sheng, D., Fredlund, D.G., and Gens, A. (2008). “A new modelling approach for unsaturated soils using independent stress variables.” Canadian Geotechnical Journal. 45(4), 511-534.

Skempton, A.W. (1960) “Effective stress in soils, concrete and rocks.” Pore Pressure and Suction in Soils, Butterworths, London, 4-16.

van Genuchten, M.T. (1980). “A closed-form equation for predicting the hydraulic conductivity of unsaturated soils.” Soil Science Society of America Journal, 44(5), 892-898.

Wayllace A., and Lu, N. (2012). “A transient water release and imbibitions method for rapidly measuring wetting and drying soil water retention and hydraulic conductivity functions.” Geotechnical Testing Journal. 35(1), 103-117.

Wheeler, S.J., and Sivakumar, V. (1995). “An elastoplastic critical state framework for unsaturated soil.” Géotechnique, 45(1), 35-53.

Zimmerman, H.D., Wagner, M.H., Carney, J.A., and Ito, Y.M. (1987). Effects of Site Geology on Ground Shock Environments: Report 1, Constitutive Models for Materials I2, I3, and W1-W10. USACE Technical Report SL-87-19. Vicksburg, MS.

LIST OF TABLE AND FIGURE CAPTIONS

Figure 1: Transitions in behavior of unsaturated, compacted soils during compression to high stresses under undrained conditions

Figure 2: Parametric evaluation of the modified Hilf analysis: (a) Pore pressure change required for pressurized saturation of soils having different initial degrees of saturation; (b) Pore pressure change during undrained loading for soils having different initial degrees of saturation; (c) Pore pressure change during undrained loading for soils having different $m_{v,u}$ values

Figure 3: SWRC with initial suctions in the compacted specimens measured using a tensiometer

Figure 4: Undrained compression behavior with different S_{r0}: (a) e-logp (b) e-p

Figure 5: Comparison of the initial air volume $V_{a,i}$ of the different soil specimens with the volume of voids at pressurized saturation $V_{v,ps}$

Figure 6: Undrained compression indices under different S_{r0}: (a) Apparent preconsolidation stress p_c; (b) Slope of unsaturated soil ($\lambda_{u,i}$)

Figure 7: Assessment of pressurized saturation for Boulder clay: (a) Pore pressure change of Boulder clay under different initial degrees of saturation; (b) Comparison of the pressurized saturation under different S_{r0} (prediction vs. experimental data)

Figure 8: Changes in the coefficient α_u with mean total stress for soil specimens having different initial degrees of saturation

Figure 9: (a) Comparison of the model predictions (dashed lines) with the experimental data (solid lines) for undrained compression of clay under different S_{r0} (e-logp); (b) Comparison of the model predictions (dashed lines) with the experimental data (solid lines) for undrained compression of clay under different S_{r0} (e-p); (c) Model predictions under different S_{r0} (e-logp); (d) Model predictions under different S_{r0} (e-p)

Table 1: Summary of results from the isotropic compression tests

Parameter	**Values**				
$\mathbf{e_0}$	0.509	0.506	0.507	0.515	0.519
$\mathbf{S_{r0}}$	1.00	0.92	0.84	0.72	0.61
$\mathbf{w_0}$	18.9*	17.3	15.7	13.8	11.8
$\boldsymbol{\kappa_{u,i}}$	0.0015	0.003	0.003	0.003	0.003
$\mathbf{p_c}$ **(kPa)**	-	280	350	480	635
$\boldsymbol{\lambda_{u,i}}$**	-	0.010	0.016	0.037	0.053
$\mathbf{p_{ps}}$ **(kPa)**	-	6,000	8,000	10,000	11,000

*Compacted at w_0 = 17.3% then saturated to 18.9% using upward flow under vacuum

** $\lambda_{u,i}$ is defined over the stress range ($p_c<p<p_{ps}$)

Table 2: Undrained compression model parameters for Boulder clay

Parameter	Value		Units
$\mathbf{e_0}$	0.51		-
$\boldsymbol{\kappa_{u,i}}$	0.00015 (S_r = 1.0) 0.003 (S_r < 1.0)		-
$\mathbf{p_c}$ **model**	A B	-852 198	kPa kPa
$\boldsymbol{\lambda_{u,i}}$ **model**	Z	-0.104	-
$\mathbf{u_{a0}}$	101.3		kPa
$\mathbf{k_h}$	5628		kPa
$\mathbf{K_w}$ **(=K)**	2.2×10^6		kPa
$\boldsymbol{\alpha_u}$ **model**	A^u	-0.7	-

Figure 1

Click here to download Figure Fig 1.tif

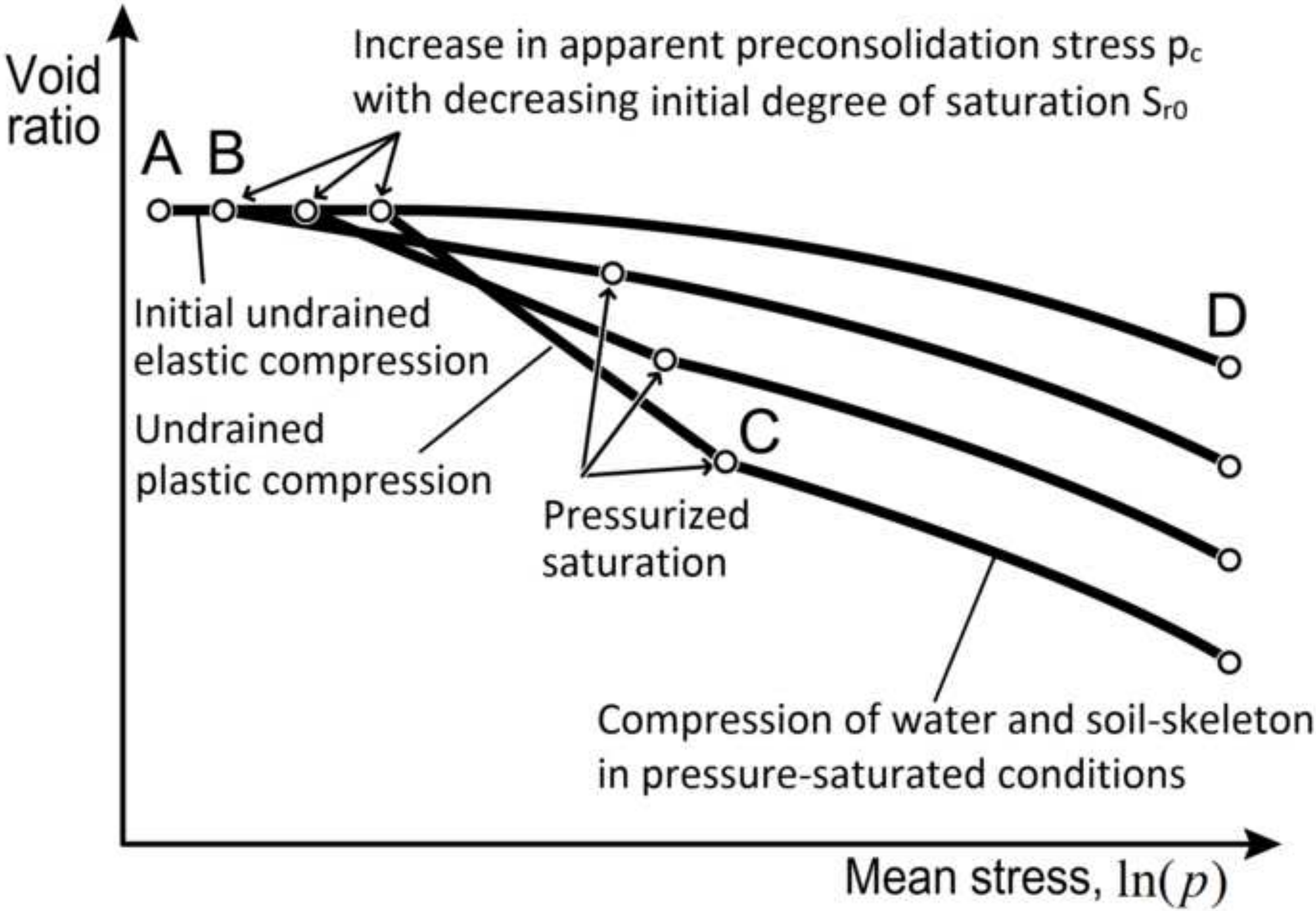

Figure 2

Click here to download Figure Fig 2.tif

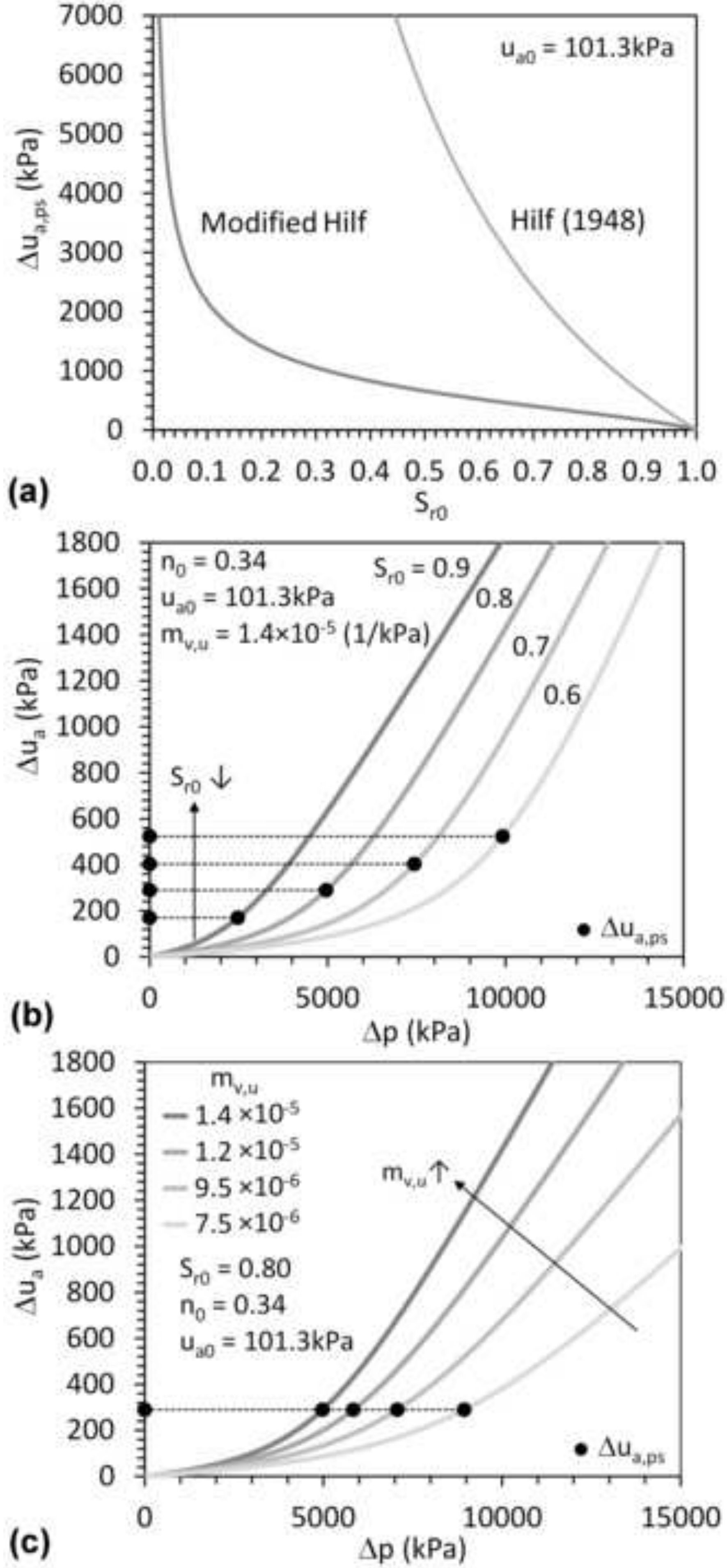

Figure 3

Click here to download Figure Fig 3.tif

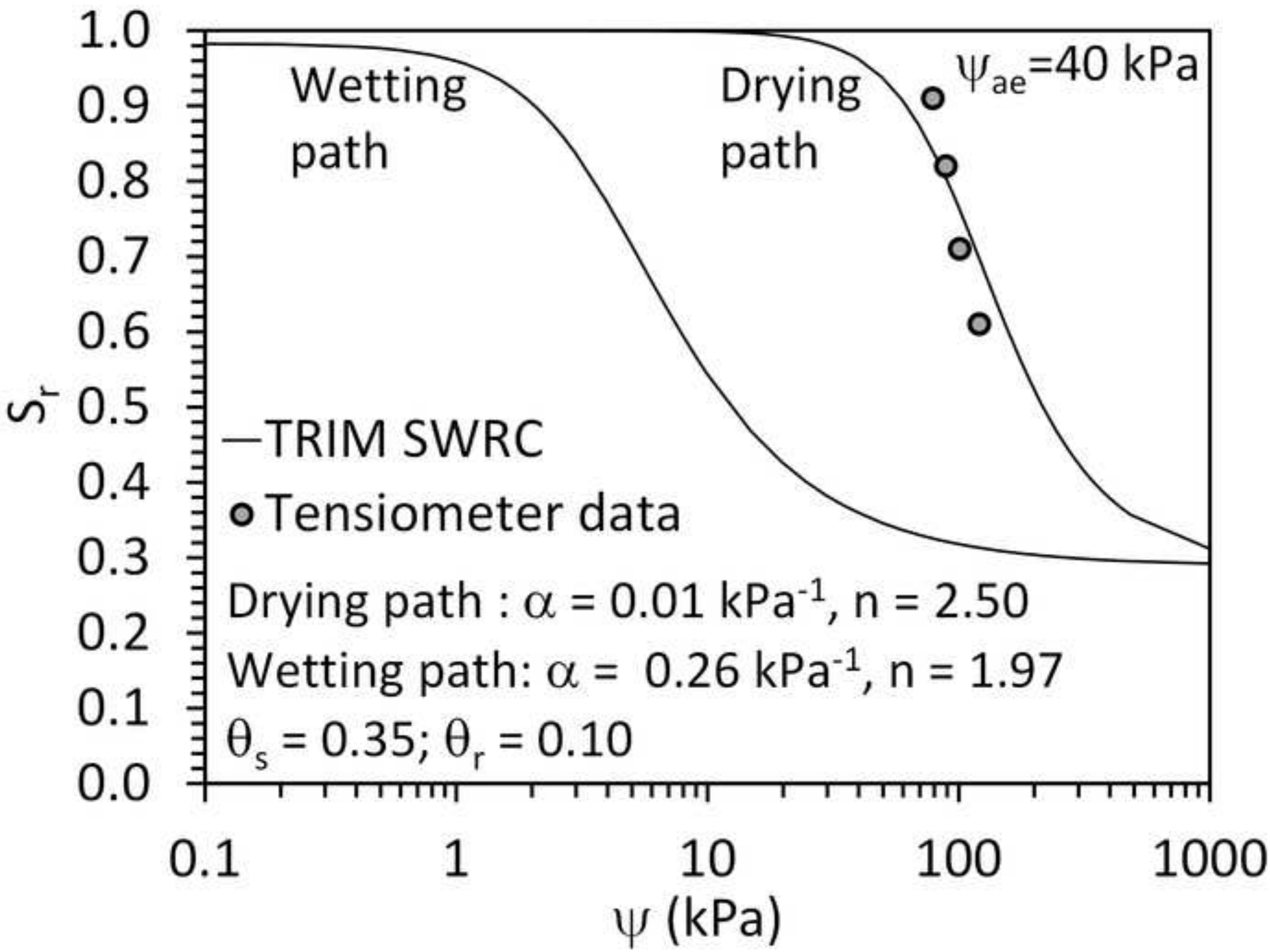

Figure 4

Click here to download Figure Fig 4.tif

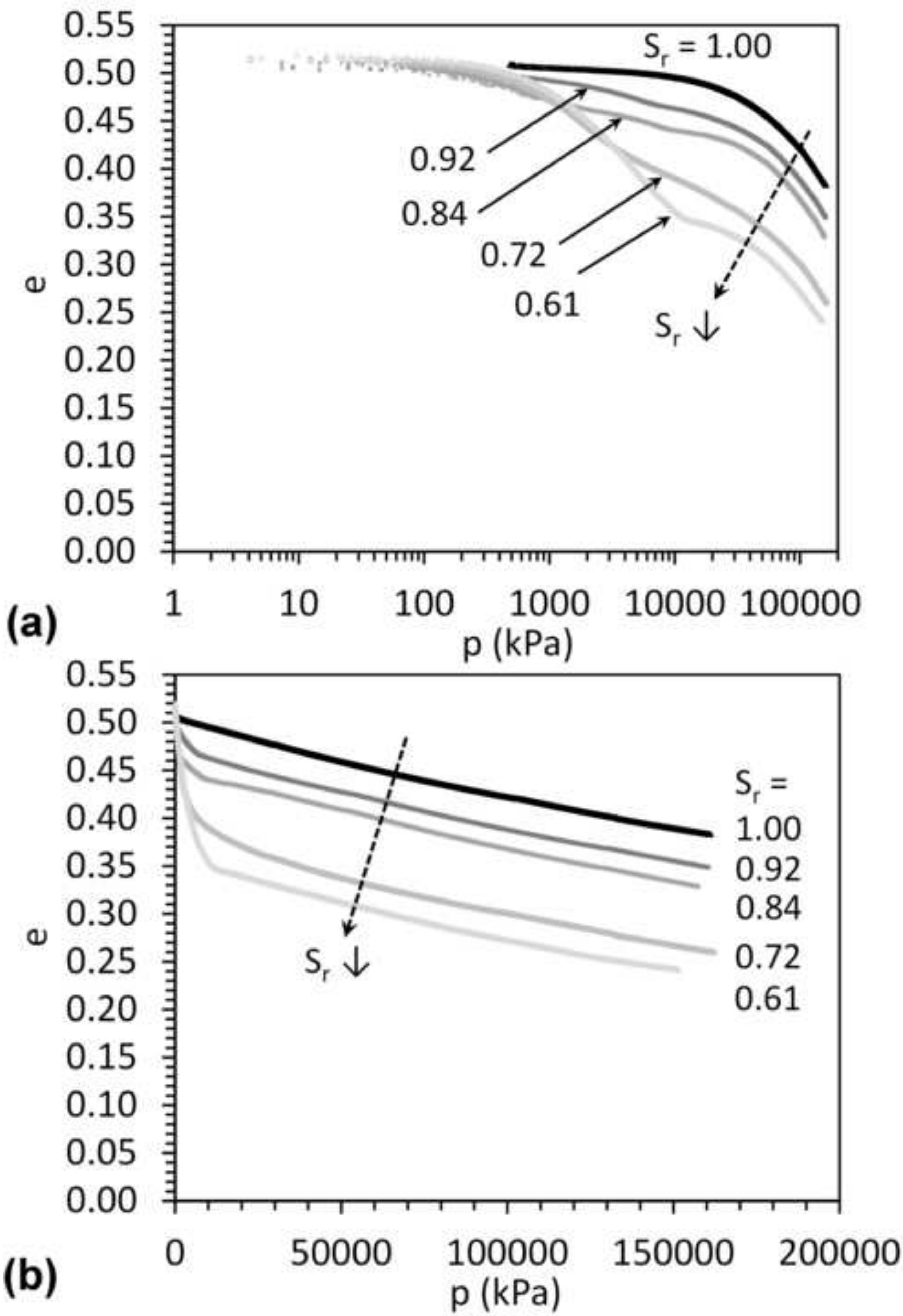

Figure 5

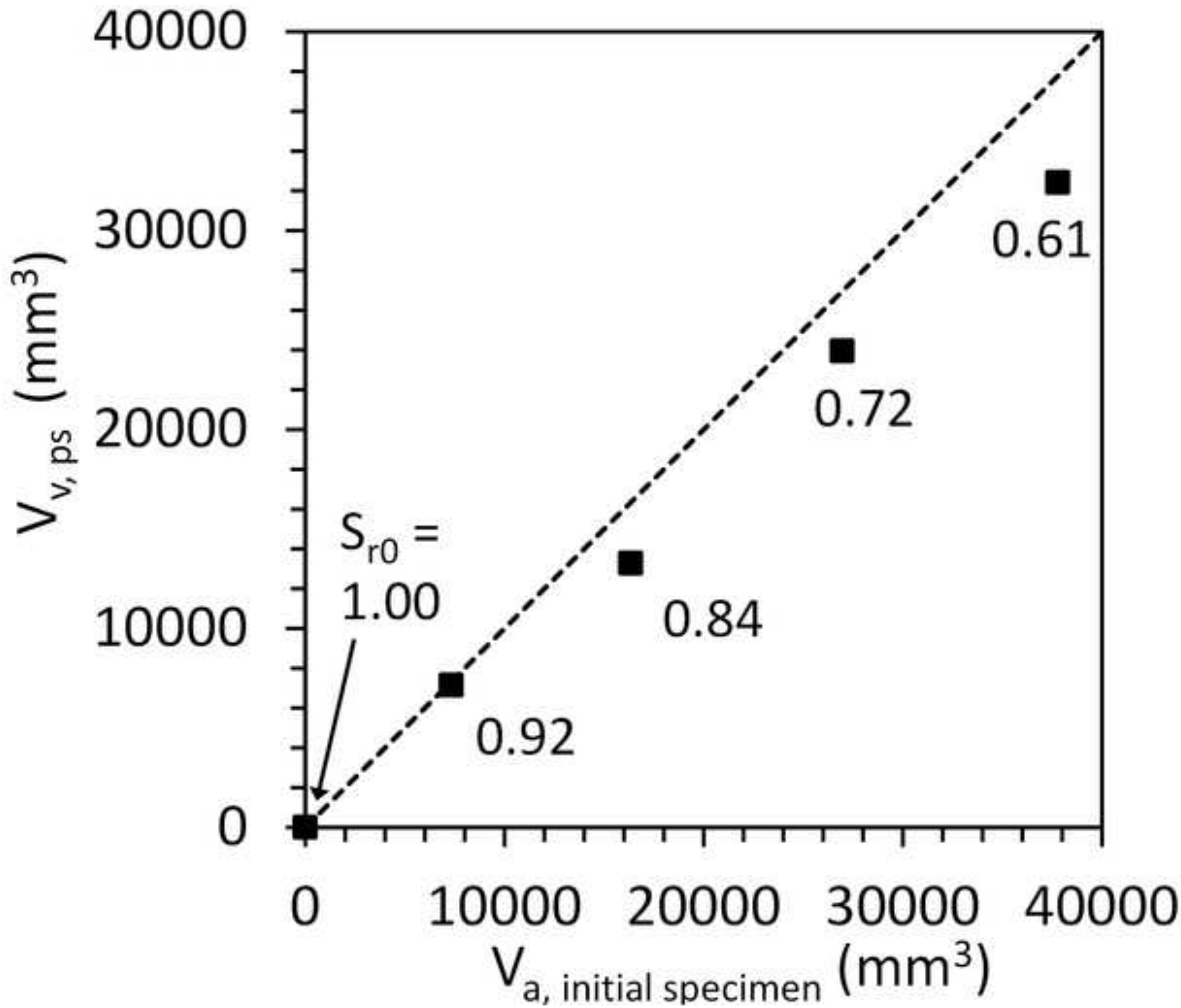
40000
30000
20000
10000
0
$V_{v, ps}$ (mm^3)
S_{r0} =
1.00
0.92
0.84
0.72
0.61
0
10000
20000
30000
40000
$V_{a, \text{initial specimen}}$ (mm^3)

Figure 6

Click here to download Figure Fig 6.tif

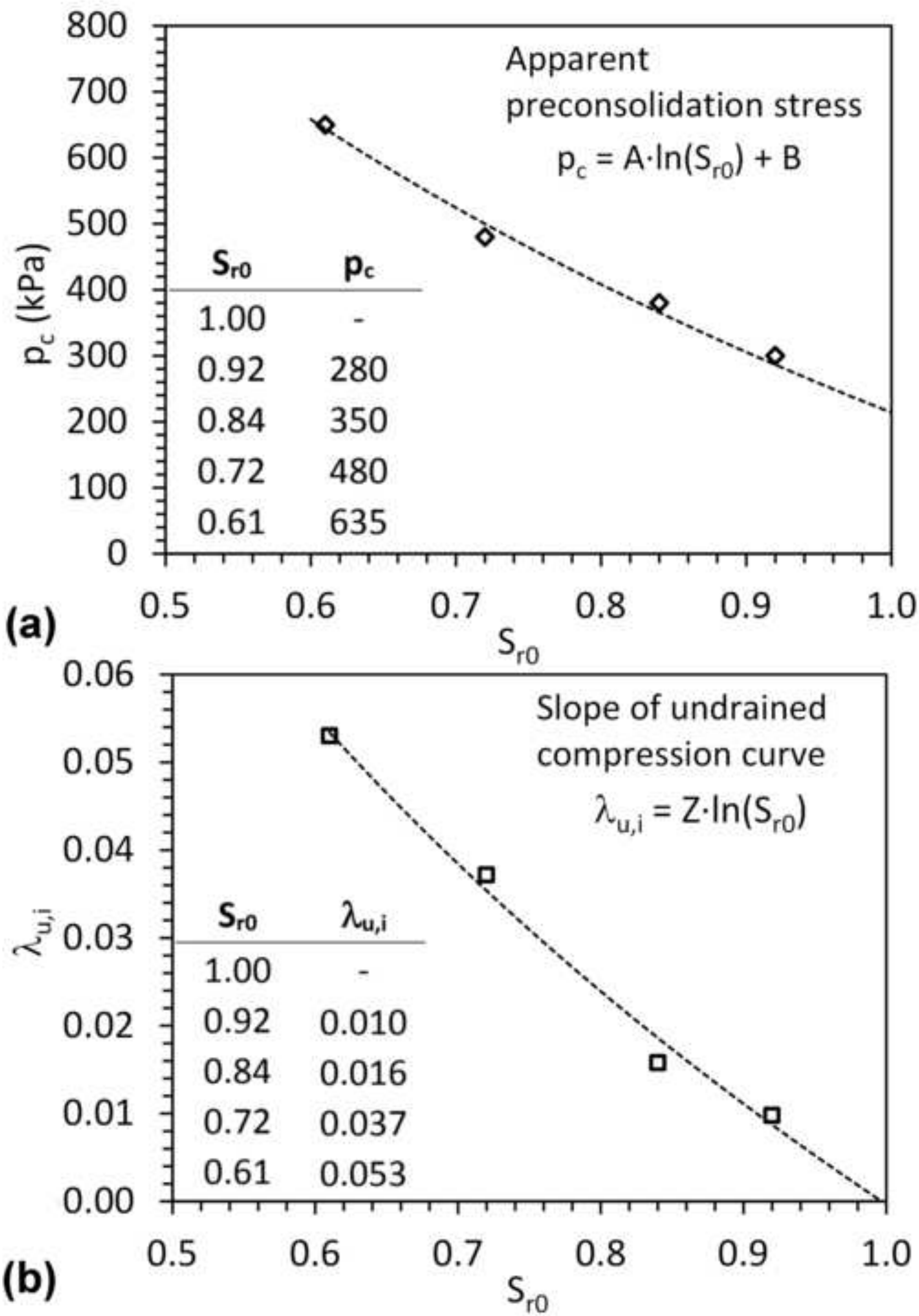

Figure 7

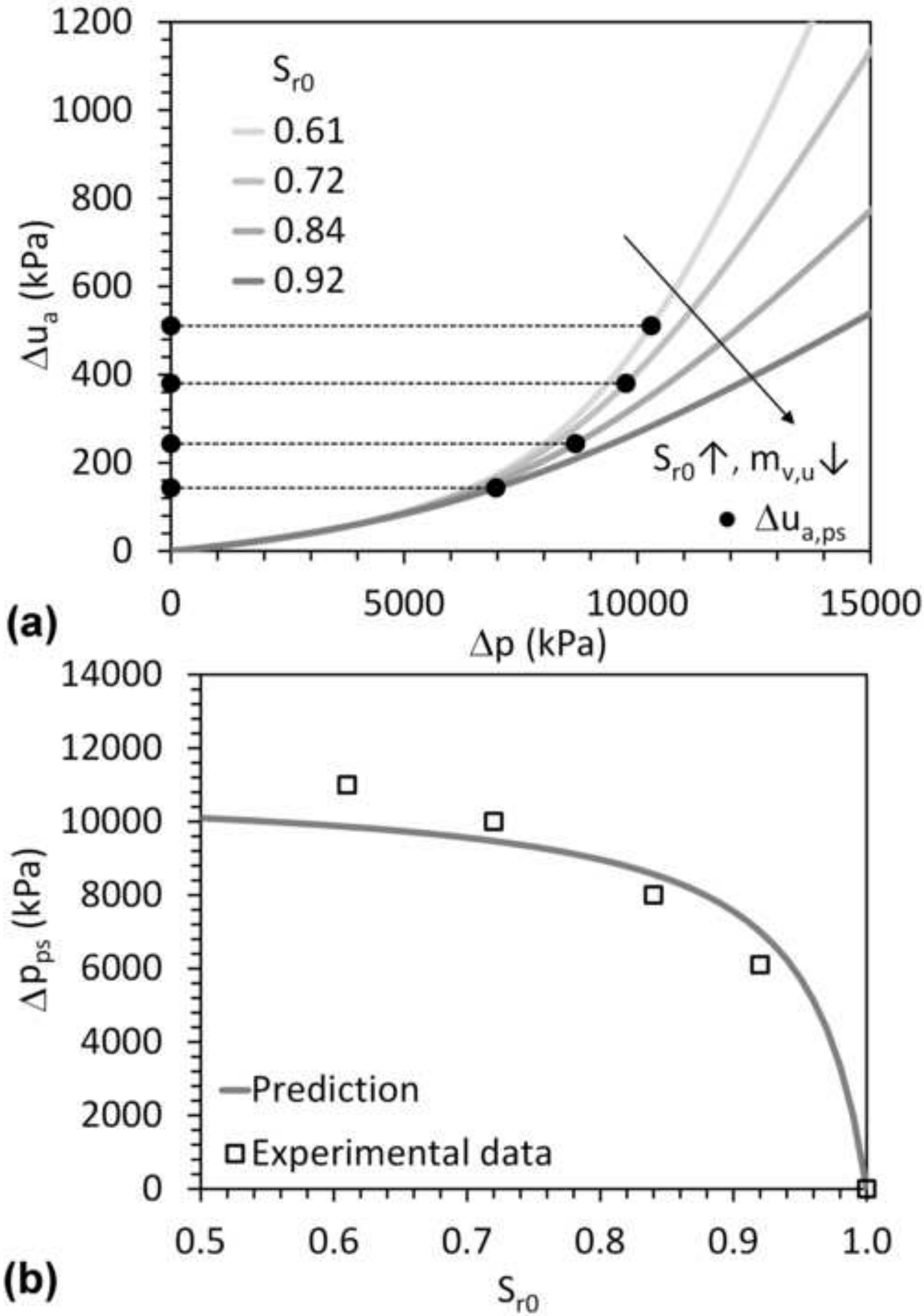

1200
1000
800
600
400
200
0
S_{r0}
0.61
0.72
0.84
0.92
Δu_a (kPa)
$S_{r0}\uparrow$, $m_{v,u}\downarrow$
$\Delta u_{a,ps}$
0
5000
10000
15000
(a)
Δp (kPa)
14000
12000
10000
8000
6000
4000
2000
0
Δp_{ps} (kPa)
Prediction
Experimental data
0.5
0.6
0.7
0.8
0.9
1.0
(b)
S_{r0}

Figure 8

Click here to download Figure Fig 8.tif

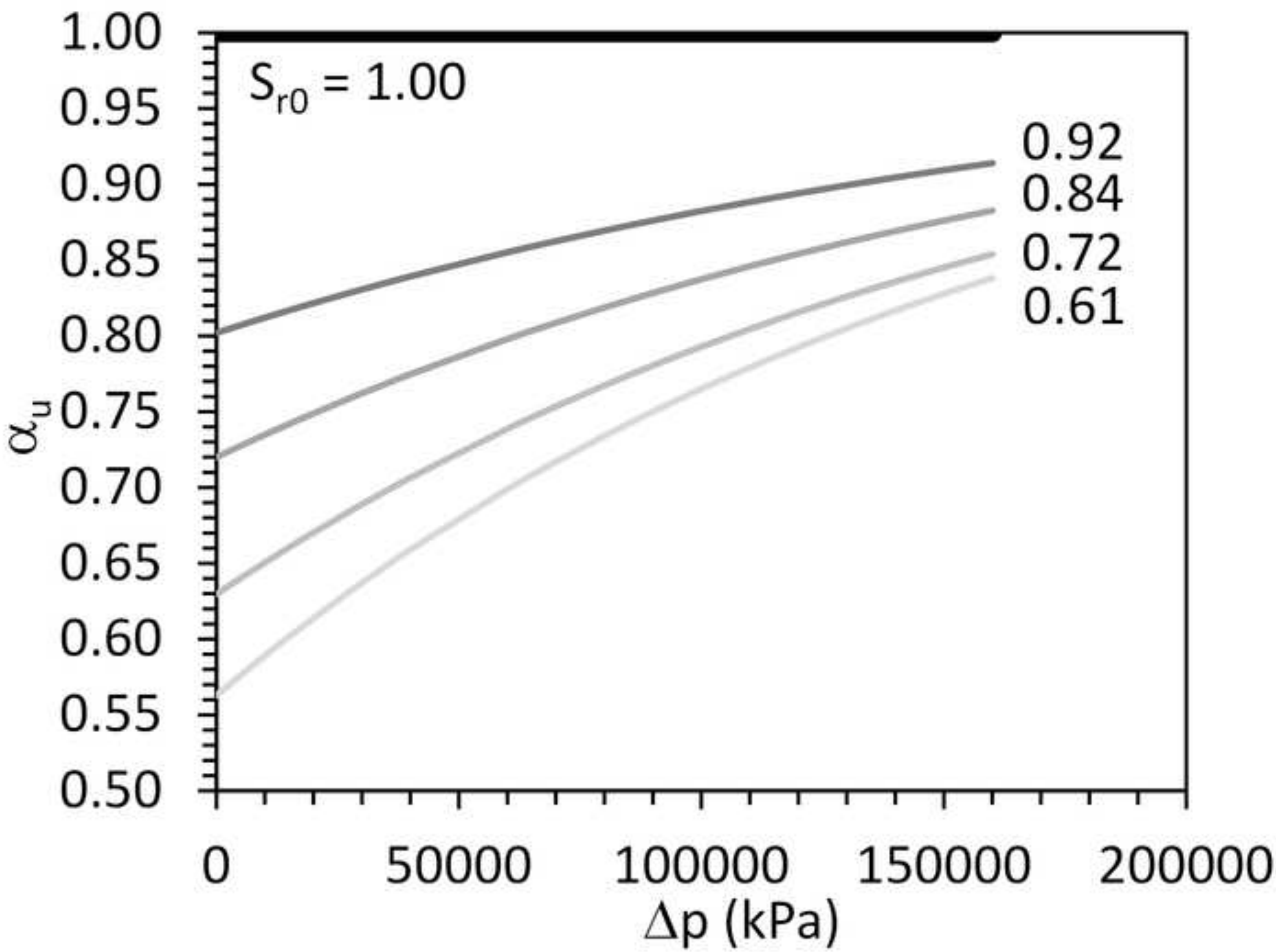

Figure 9

Click here to download Figure Fig 9.tif